Materials Today: Proceedings 33 (2020) 1444–1452

Contents lists available at ScienceDirect

Materials Today: Proceedings

journal homepage: www.elsevier.com/locate/matpr

A simple synthesis of ZnO:Co_2O_3 nanocomposites by pulsed laser irradiation in liquid

Sreed Sharma Kanakkillam [a], Bindu Krishnan [a,b], David Avellaneda Avellaneda [a], Sadasivan Shaji [a,b,*]

[a] Facultad de Ingeniería Mecánica y Eléctrica, Universidad Autónoma de Nuevo León, San Nicolás de los Garza, Nuevo León 66455, Mexico

[b] Centro de Innovación, Investigación y Desarrollo en Ingeniería y Tecnología (CIIDIT)- Universidad Autónoma de Nuevo León, Parque de Investigación e Innovación Tecnológica (PIIT), Apodaca, Nuevo León 66600, Mexico

ARTICLE INFO

Article history:
Received 30 June 2020
Accepted 20 August 2020
Available online 24 September 2020

Keywords:
Nanocomposites
Zinc oxide
Cobalt oxide
Pulsed laser irradiation in liquid
XPS
Photocatalysis

ABSTRACT

Nanocomposite materials are emerging in popularity due to their enhanced performance over the constituent materials. In this work, we report the fabrication of zinc oxide: cobalt oxide nanocomposites in a simple, fast and room temperature synthesis with good productivity. The nanocomposites synthesized were characterized by SEM, XPS and UV–Visible spectroscopy to analyze their morphology, composition, chemical states, optical absorption, band gap etc. The nanocolloids of the composite were drop casted to form thin films for photocatalytic studies. In SEM analysis, the morphological transformation of the material is observed where it transformed from agglomerated spherical particles to petals shaped and then to partially spherical forms due to pulsed laser irradiation. XPS analysis showed a gradual change in oxygen high resolution spectra in the samples with respect to the concentration difference of cobalt oxide. The optical studies show an enhanced absorption in visible region for the nanocomposite and the energy band gap reduced to 2.4 eV. All the thin films of nanocomposite showed photocatalytic decay of methylene blue dye under visible light irradiation. The results of this study support the effective use of laser irradiation in liquid to obtain nanocomposites of metal oxides for photocatalytic applications.

Selection and peer-review under responsibility of the scientific committee of the International Conference on Photochemistry and Sustainable Energy (ICPSE 2019).

1. Introduction

Metal oxide materials have increasing demand in the scientific community due to their eco-friendliness, stability, natural abundance, ease of synthesis, and wider application purposes. Different types of metal oxides and their nanomaterials are being used in an extensive variety of fields like adsorbents, gas sensors, photovoltaics, photoelectronic, and electrochemical, fuel cells, ceramics and other biological applications[1]. Recently, a study is reported with SiO_2 nanomaterials for virus resistive, reusable masks like COVID-19[2]. Most of the metal oxides are categorized under semiconductors. Semiconductors can be considered as a partial conductor or partial insulator, which can be made a conductor by tuning its properties. Generally, most of the metal oxide materials are being used in the fields of photovoltaics, energy storage devices, photocatalysis etc.[1]. The common metal oxides are that of metals like Ti, Zn, Co, V, Fe etc. having optical band gap energies in the range of 1 to 3.5 eV approximately[3]. Hence, tuning the parameters of synthesis, modifications of morphology as well as some treatments for the materials will be able to make them ready for better photon energy related applications, like photovoltaics and photocatalysis.

The metal oxide semiconducting materials can be tuned for their properties with the help of other metals, metal oxides etc. There are studies in which metal oxides were modified to nanocomposites or hybrid materials and they exhibited better properties than that of the regular metal oxides. TiO_2 and ZnO are two well explored metal oxide materials in different applications of material science particularly that of metal oxide semiconductors and optoelectronics. The band gap of these materials is almost similar, ~3.3 eV[4,5]. This wide band gap energy, which is near UV and closer to the end of the blue spectral region enables these materials to be tuned, so that they can absorb the visible photon energy of the solar spectrum. ZnO has a band gap of 3.3 eV so that this range can absorb the UV region only of the solar

* Corresponding author at: Facultad de Ingeniería Mecánica y Eléctrica, Universidad Autónoma de Nuevo León, San Nicolás de los Garza, Nuevo León 66455, Mexico.

E-mail address: sadasivan.shaji@uanl.edu.mx (S. Shaji).

https://doi.org/10.1016/j.matpr.2020.08.533
2214-7853/
Selection and peer-review under responsibility of the scientific committee of the International Conference on Photochemistry and Sustainable Energy (ICPSE 2019).

spectrum. There are many reports available in literature which show modifications of zinc oxide with other metals and metal oxides[6–9]. These researches show better application results, and which urge us to focus on a related investigation. Our previous work with zinc oxide and cobalt oxide showed better photocatalytic efficiency than the normal zinc oxide and cobalt oxide[10].

Laser based synthesis techniques, especially pulsed laser ablation in liquid (PLAL) is recognized as a unique single step method for synthesizing nanomaterials. Most of the product materials by PLAL are of the same composition and phase as that of the target material with a different size, physical and chemical properties etc. This technique has been used frequently for the synthesis of metal nanoparticles, oxide nanomaterials, ceramic nanoparticles, chalcogenide nanomaterials etc. in different organic and inorganic liquid media[11–13]. Another laser based technique, pulsed laser irradiation/fragmentation is used for the modification of micro and nano materials. The micro and nano materials under pulsed laser fragmentation can be intensively used to change properties of the materials in a better way. Our group modified TiO_2 to black TiO_2 with the help of pulsed laser irradiation of white TiO_2 dispersed in water using 532 nm laser output [14]. In our previous work, we successfully synthesized and characterized the structure, morphology, optical photocatalytic properties of zinc oxide cobalt oxide nanoflakes from cryomilled zinc oxide and cobalt oxide powders[10]. Also, stable nanocolloids of cobalt oxide were prepared in water using pulsed laser fragmentation in liquid[15]. Thin films of Co_2O_3 were fabricated by spray deposition and their photocatalytic properties were studied.

Photocatalysis, nowadays boosts its popularity due to the increasing level of contaminants in nature. It is the purpose to invent better photocatalytic materials for reduction of environmental pollutants including those in air, water, and soil. A photocatalyst can help for the purification of nature as dye decay, anti-pollutants, self-cleaning mechanism etc.[16–18]. Photocatalysts can used in the areas of cleaner and renewable energy through hydrogen evolution reactions, water splitting reactions which will reduce the CO and CO_2 emission from biofuels by replacing them [19,20]. In biological applications, photocatalysts can be used for anti-bacterial applications, sterilization applications etc.[21,22]. Metal oxides like, TiO_2 and ZnO are two well explored photocatalysts[23–25]. The materials (photocatalysts) morphology, size, optical properties can be tuned by different synthesis techniques and by the addition of other materials. In this work, we synthesized zinc oxide: cobalt oxide nanocomposites in a very simple synthesis by pulsed laser irradiation in water technique. These nanocomposites are characterized for their morphology, composition, optical properties and their thin films prepared from the nanocolloids are used for photocatalytic studies.

2. Experimental

2.1. Materials

Zinc oxide was purchased from Shanghai Hansi Chemical Industry Ltd, China (99.9% purity), cobalt oxide from Tianjin Guangzhou Chemical Research Institute, China (99.9% purity), and methylene blue dye from Atom Scientific, United Kingdom.

2.2. Synthesis of cobalt oxide nanocolloid

Nanocolloid of cobalt oxide (Co_2O_3) was prepared by pulsed laser fragmentation in liquid technique. This was produced by laser irradiation of Co_2O_3 dispersed in deionized water. To produce this colloid in water we followed the same procedures of our previous work[15]. Here we used 1.5 mg of Co_2O_3 powder in 10 ml of distilled water. The weighed cobalt oxide powder was dispersed in distilled water and the mixture was sonicated to get uniform dispersion of the powder. After sonication process, the mixture was stirred continuously and irradiated horizontal position using the nanosecond pulsed Nd:YAG laser output (260 mJ/pulse, fluence of 0.33 J/cm^2 and a wavelength of 532 nm). After 25 min of irradiation, the mixture was turned to a stable, uniform, yellowish, cobalt oxide nanocolloid in distilled water.

2.3. Synthesis of zinc oxide-cobalt oxide nanocomposites

Zinc oxide powder was weighed and added to the cobalt oxide nanocolloid. This colloidal mixture was sonicated for 10 min. Then the mixture appeared brownish. This mixture was stirred and irradiated with pulsed laser output. The irradiation process lasted for 20 min and the solution turned greenish. To get different concentrations of this composite, different quantities of zinc oxide were taken, 30 mg, 60 mg, and 90 mg. The produced zinc oxide- cobalt oxide nanocomposites were with different percentages of cobalt oxide, 1.7%, 2.5% and 5%. These samples were named as CZ1, CZ2 and CZ5. For photocatalytic studies, each of the powders obtained the nanocomposite were dispersed in isopropyl alcohol and drop casted to a glass substrate of size 2×4 cm. 2.5 mg of the nanocomposite powder was taken from each sample (CZ1, CZ2 and CZ5) for the preparation of drop casted thin films.

2.4. Characterization

A scanning electron microscope, Hitachi SU 8020 was used for morphological studies in secondary electron mode using an acceleration voltage of 1 kV. XPS analysis was carried out using a Thermo Scientific K-alpha X-ray photoelectron spectrometer, with a monochromatized Al Kα radiation with hυ = 1486.88 eV. Using XPS, elemental identification and chemical states of the elements were analyzed. UV–Visible-NIR spectrophotometer (Jasco V-770) with an integrating sphere system was used for optical studies. The integrating sphere was used to measure the diffused reflectance spectroscopy of the powder samples. For measuring the catalytic photodegradation, the absorption spectra were collected by the same spectrophotometer at regular intervals of irradiation.

2.5. Photocatalysis

For photocatalytic studies, we followed the common organic dye decay method. Methylene blue (MB), a well explored textile dye was used as the colorant. The drop-casted glass thin film was placed inside a 30 ml beaker and 15 ml dye- water solution was added to it. The concentration of methylene blue dye in water was 5 mg/L. We kept on stirring the solution in a dark environment for uniform distribution of the dye to check if there is any dye decay in dark condition for 15 min. A solar simulator of 200 W was used as the light source for the photocatalytic experiment. The simulator light was irradiated after 15 min under the dark conditions. Then in every 15 min during light illumination, sample from the dye-water solution was taken for absorption measurement. The dye decay rate was analyzed by evaluating the percentage of dye removed in every 15 min for 90 min in total. Dye decay for all samples was studied in this manner and the results are analyzed.

3. Results and discussion

3.1. Pulsed laser irradiation

The details of the synthesis of stable cobalt oxide nanoparticles in distilled water and the mechanism involved were explained in our previous work [15]. A photo of the metal oxides as precursors and the nanocolloid of Co_2O_3, as well as their nanocomposite obtained by laser irradiation, are shown in Fig. 1. A photo of the cobalt oxide is shown in Fig. 1(a) and that of zinc oxide in Fig. 1 (c). The stable cobalt oxide nanocolloid obtained by laser irradiation of Co_2O_3 in water is shown in Fig. 1(b). We have already reported the synthesis and photocatalytic studies of zinc oxide: cobalt oxide nanocomposite by cryomilling assisted pulsed laser fragmentation technique[10]. So, here we are using the procedure of nanocomposite synthesis in a different way. After the preparation of stable nanocolloid of Co_2O_3, zinc oxide powder was added to it. At the time of addition of these powders, it was appeared to be drowning in the colloid slowly. Under sonication, the powder got well dispersed in the colloid and the colloidal mixture appeared partially brown, which is shown in Fig. 1(d). When the zinc oxide powder in cobalt oxide nanocolloid mixture was irradiated using a pulsed laser source, laser fragmentation occurred for the nanomaterials resulting in a greenish nanocolloid (Fig. 1(e)). At the initial stage, the whole mixture was stirred, and the pulsed laser was irradiated to it in a horizontal configuration. Here the synthesis part is at room temperature and productivity of these nanocomposites were increased approximately 10 times over the previously reported method in a much easy and rapid way. Thin films of these nanocomposites were prepared by drop casting the nanocolloids on glass substrates and their photocatalytic studies were carried out.

The laser wavelength was of 532 nm, so that the cobalt oxide nanoparticles have more probability to absorb photon energy, due to the energy band gap of the material. Even considering that aspect, the maximum concentration of cobalt oxide was 5% only. Hence, in this case, the zinc oxide nanoparticles also contributed to the photon energy absorption leading to heating, melting and fragmentation process. During the laser irradiation, the laser beam also interacts with the zinc oxide powder due to the abundance of zinc oxide and their morphology like agglomerated spherical particles could have supported the photon absorption. The absorbed photon energy will be transferred to electrons first, then to the lattice. This will heat the overall material and laser melting will occur [5]. At the same time, the excess energy will cause a mechanical fragmentation of the particles in the mixture. By this procedure, the materials in the mixture will undergo laser melting and fragmentation in the presence of colloidal cobalt oxide nanoparticles. The fragmented and molten zinc oxide then combines with the cobalt oxide nanoparticles present in the colloidal medium. This will transform the property of zinc oxide and cobalt oxide into a unique one, that is of the nanocomposites. The resulted nanocomposite color (Fig. 1(e)) shows the effect of laser irradiation where the morphology and size modification due to laser fragmentation ensuing in modified optical properties. After the laser irradiation, the powder got settled at the bottom of the beaker and the water appeared to be partially transparent. This indicated that the zinc oxide in cobalt oxide colloid was completely transformed and their nanocomposites were formed.

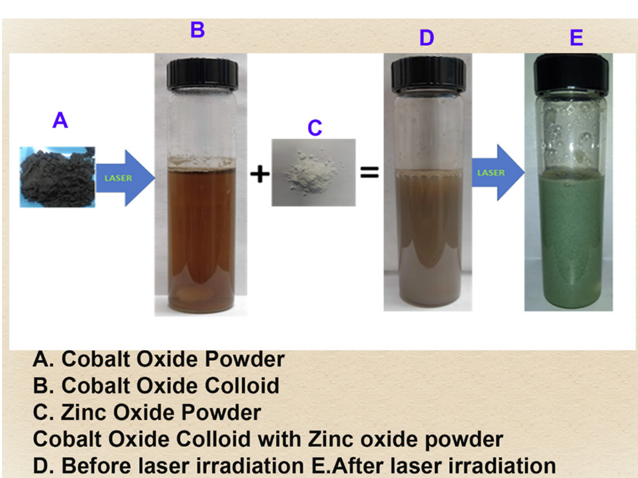

Fig. 1. Steps of zinc oxide - cobalt oxide nanocomposite synthesis.

In Fig. 2, the product nanomaterials, zinc oxide: cobalt oxide nanocomposites (CZ) with different percentages of cobalt oxide is shown. From these figures, it can be understood that the color of the product nanomaterial is changing in accordance with the increase in concentration of Co_2O_3. The nanocomposite samples obtained by laser fragmentation are CZ1, Fig. 2(a), is the sample with 1.7% of cobalt oxide, CZ2, Fig. 2(b), is the sample with 2.5% of cobalt oxide, and CZ5, Fig. 2(c), is the sample with 5% of cobalt oxide. The color of CZ1 is slightly greenish while CZ5 is dark green, and this can be considered in another view that the zinc oxide quantity is higher in CZ1 and lower in CZ5.

3.2. Morphological studies

Scanning electron microscopic images were used for the morphological analysis of the nanocomposite samples. The images were taken using secondary electrons so that the dark and bright parts of the images indicated the height difference of the samples. Fig. 3 includes the SEM images of the nanocomposites obtained. In our previous studies with the precursor materials, the morphology of zinc oxide was observed as agglomerated spherical particles and the cobalt oxide material has rod like morphology[15]. In Fig. 3 (a, b) the morphology of the CZ1 sample is given. It appears to be of non-uniform shapes. From the image, it can also be understood that the samples were like different shaped particles attached together. The rapid cooling effect caused by the liquid environment might be the reason for this. In CZ1, the amount of zinc oxide is higher, and this also might be a reason for the agglomerated structure because the morphology of ZnO was of agglomerates of spherical particles. In the case of CZ2, the morphology has a significant change from that of CZ1. The morphology of CZ2 samples is shown in Fig. 3. (c, d), and it is observed like flower petals shape. This can be evidently witnessed at higher magnification image of the sample given in Fig. 3(d). The surface morphology of the sample CZ5 is available in Fig. 3(e, f). From these images, the morphology is changed to more spherical due to the laser irradiation. In the images, we can observe majority areas of spherical particles with some needle like structures.

While comparing the morphology of these nanocomposites with our previous work, the morphology has a significant difference. The cryo-milled assisted pulsed laser fragmentation of zinc oxide and cobalt oxide provided different types of nanoflakes [10], whereas here in this work we observed a gradual change in morphology, that is agglomerated particles to petal shaped and then to spherical particles. In the literature, we can observe some works related to the nanocomposites of zinc oxide and cobalt oxide. Zhang et al. synthesized ZnO-Co_3O_4 nanocomposites by chemical method for acetone sensing applications in which they obtained a morphology of hollow polyhedron shape[26]. In another work with Co metal and zinc oxide, the morphology appeared as core–shell [27]. They produced these materials using UV irradiation of a mixture with zinc oxide and cobalt nitrate. In this work, the laser irradiation of nanocolloids of ZnO:Co_2O_3 showed different morphology than the earlier reported ones. Morphological changes were observed for each nanocomposite according to the concentration of Co_2O_3 present under the irradiation process.

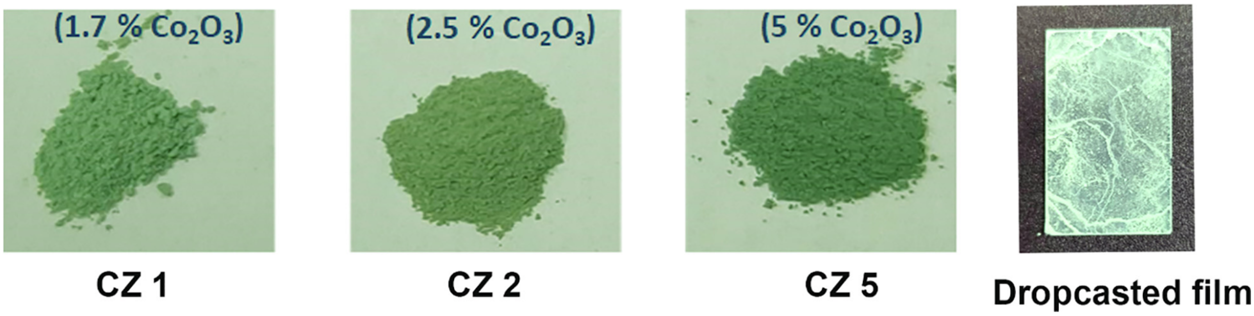

Fig. 2. Photographs of CZ samples with different concentrations of cobalt oxide and the drop casted thin film.

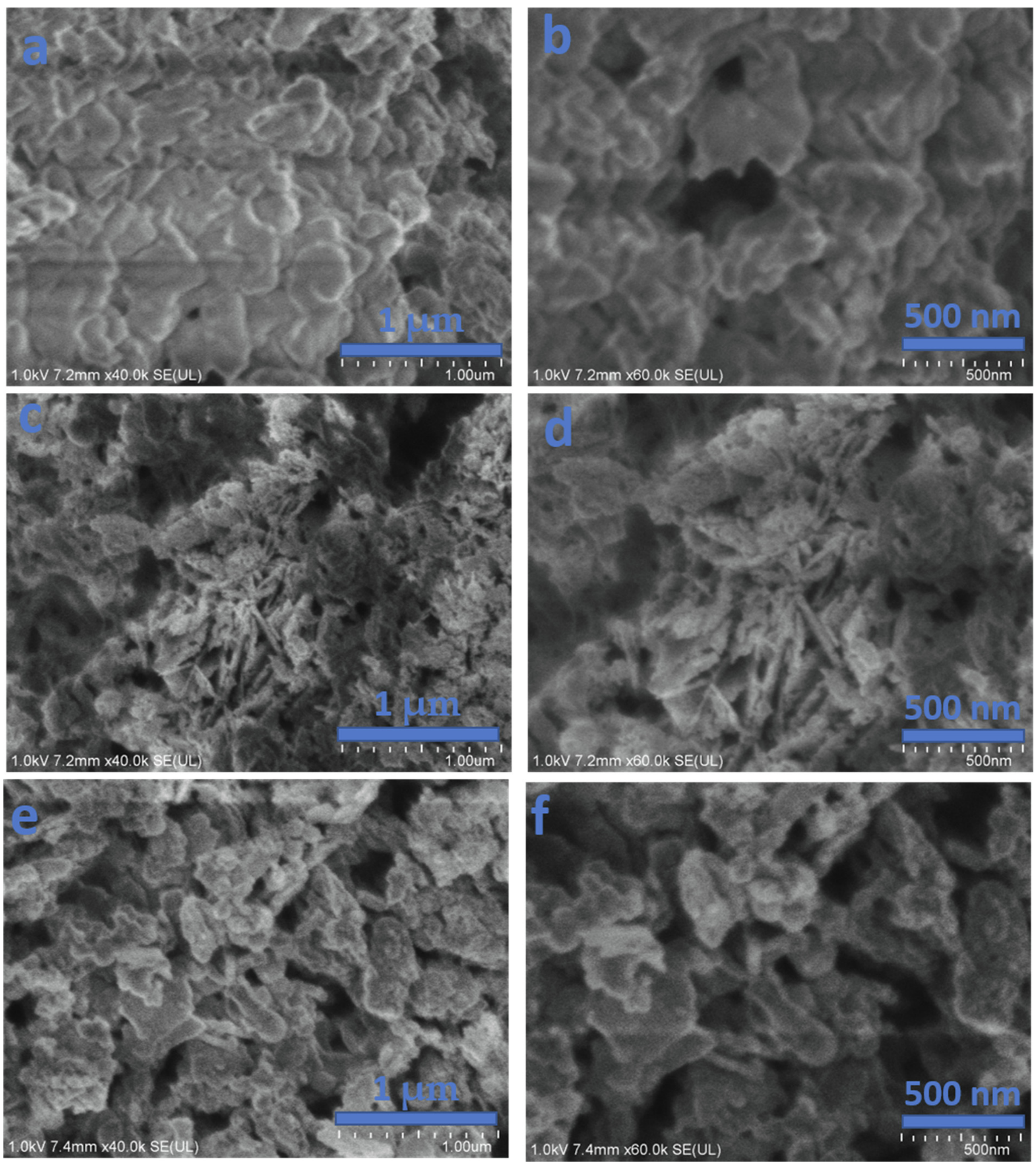

Fig. 3. Scanning electron microscopic images of the samples (a, b) CZ1, (c, d) CZ2, (e, f) CZ5.

3.3. X-ray photoelectron spectroscopy (XPS)

From the X-ray photoelectron spectroscopy analysis, the elemental compositions of the samples were identified. A survey spectral analysis (low resolution photoelectron spectra with pass energy of 200 eV) was first done to identify the elements present on the sample surface. There were no contaminations/foreign elements detected on the sample surfaces, so there was only the presence of Zn, Co, O, and C (adventitious carbon). To know their chemical and electronic states, photoelectron spectra at high resolution (pass energy of 50 eV) were collected and analyzed. In Fig. 4 the XPS high resolution spectra of the elements are given for the three nanocomposite samples. All the spectral binding energies were standardized with photoelectron peak of adventitious carbon 1 s value of 284.6 eV. While comparing the spectra of each element in high resolution analysis, the spectra for Zn remain the same in all samples. The Zn 2p peaks are identified at 1021 and 1044 eV corresponding to the doublet of Zn 2p (Zn $2p_{3/2}$ and Zn $2p_{1/2}$ and their exact binding energy values are noted in the figure). These doublets maintained the intensity ratios of 2:1 and the binding energy difference was observed as 23 eV which matches with the reported values of zinc peaks in zinc oxide samples[4,10,28]. In the case of cobalt high-resolution spectra, according to the increase in Co_2O_3 concentration, the spectra appeared with lesser noise. Photoelectron spectra of Co 2p were observed in all the three samples and peaks were fitted for analysis. The peak positions of Co 2p doublet spectra were at 780 and 795 eV (Co $2p_{3/2}$ and Co $2p_{1/2}$, their exact peak values are given in the figure) with a binding energy difference of 15 eV approximately, which is matching with the values in the literature[10,15,29]. This difference is identified from the cobalt high-resolution spectra in Fig. 4. The additional satellite peaks observed in the high-resolution spectra are known as energy loss peaks that are well identified for cobalt photoelectron spectral analysis. In the case of oxygen, the difference in ratios of ZnO and Co_2O_3 shows slight differences for higher concentrations of Co_2O_3. The sample CZ1 contains less cobalt oxide and in this sample, the oxygen peak was not much broader. The oxygen 1 s sharp peaks observed in samples around 530 eV, which region was reported for metallic oxygen peaks in literature[10]. During the deconvolution process, there appears two peaks convolve the main photoelectron peak. These two peaks, the major peak at 529.7 eV corresponds to oxygen from zinc oxide and the other one at 530.8 eV for oxygen from adventitious oxygen. In the case of CZ2 and CZ5 oxygen high resolution peaks, there are contributions from oxygen of zinc oxide and cobalt oxide that lead to a higher FWHM (full width at half maximum) compared to that of CZ1. Among the deconvoluted peaks, the major peak at 530 eV corresponds to O^{2-} of ZnO, the other lower intensity peak at 528.9 eV corresponds to O^{2-} of Co_2O_3 as well as oxygen adsorbed on the surface at 531 eV. From XPS high resolution spectral analysis, it is evident that the concentration difference of cobalt oxide is reflected in the photoelectron spectra of the nanocomposite materials. The survey analysis and high resolution results confirmed the elemental composition and their chemical states of these nanocomposites.

The XPS analysis of our previous work with zinc oxide and cobalt oxide, the binding energy values of Zn and Co agree with

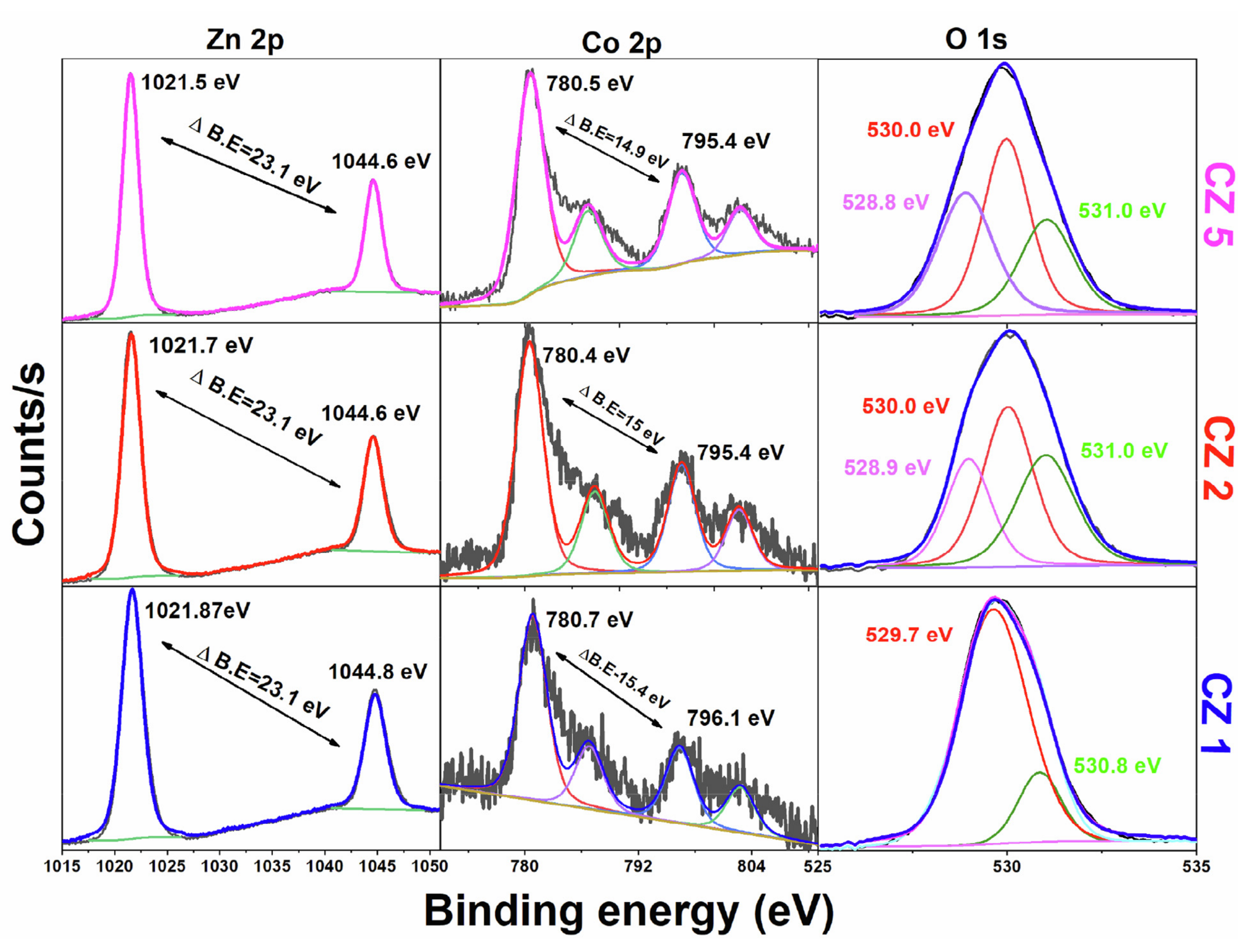

Fig. 4. XPS high resolution spectra of Zn 2p, Co 2p and O 1 s.

the current work[10], while there is some difference in the oxygen spectra. There were differences in the form of the oxygen spectra in accordance with cobalt oxide percentage. In the current work, we observed a small change whereas in previous work it was similar because of the higher concentrations of Co_2O_3 used. In both works the binding energy difference for Zn and Co doublet peaks were almost the same, that is ~ 23 eV for Zn and ~ 15 eV for Co. Another group synthesized zinc oxide and cobalt oxide nanostructures and used for photoelectrochemical studies[30] in which XPS analysis of the sample before and after PEC studies were included. They observed that the satellite peak of cobalt and the oxygen peaks were reduced after PEC studies. They observed two types of cobalt oxide and during the PEC experiment, it converted to one type of cobalt oxide, Co_3O_4.

3.4. Optical properties

The optical properties of the precursors (ZnO and Co_2O_3) and nanocomposites were studied by measuring their diffused reflectance spectra (DRS). This technique is mainly used to measure reflectance spectra from solid samples, especially powders. We plotted the absorbance spectra and evaluated the bandgap using diffused reflectance spectral data. The DRS spectra of ZnO, Co_2O_3 and the nanocomposites (CZ1, CZ2 and CZ5) prepared are shown in Fig. 5(a). From the graph, it can be seen that zinc oxide sample was highly reflective, whereas cobalt oxide was very less reflective. The reflectance spectra of the nanocomposites, CZ1, CZ2, CZ5, lie in between that of zinc oxide and cobalt oxide.

In Fig. 5 (b), the absorbance spectra are shown. The equation used for the conversion from reflectance data to absorbance is given below as

$$A = log\left(\frac{1}{R}\right) \tag{1}$$

In equation (1), A indicates the absorbance of the sample and R indicates the reflectance of the sample. From the absorbance spectra it can be understood that the nanocomposites synthesized have behaviors combined both from zinc oxide and cobalt oxide. In the case of nanocomposites, the intensity of peaks seems to be different even though the peak positions are almost the same.

To analyze closely the optical energy absorption behavior of these nanocomposites, the band gap calculations were performed using Kubelka-Munk equation[31]. It is a theoretical method for the calculation of energy band gap. Usually this method is used for powder/solid samples. The equation is given below in equation (2).

$$F(R) = \frac{(1-R)^2}{2R} \tag{2}$$

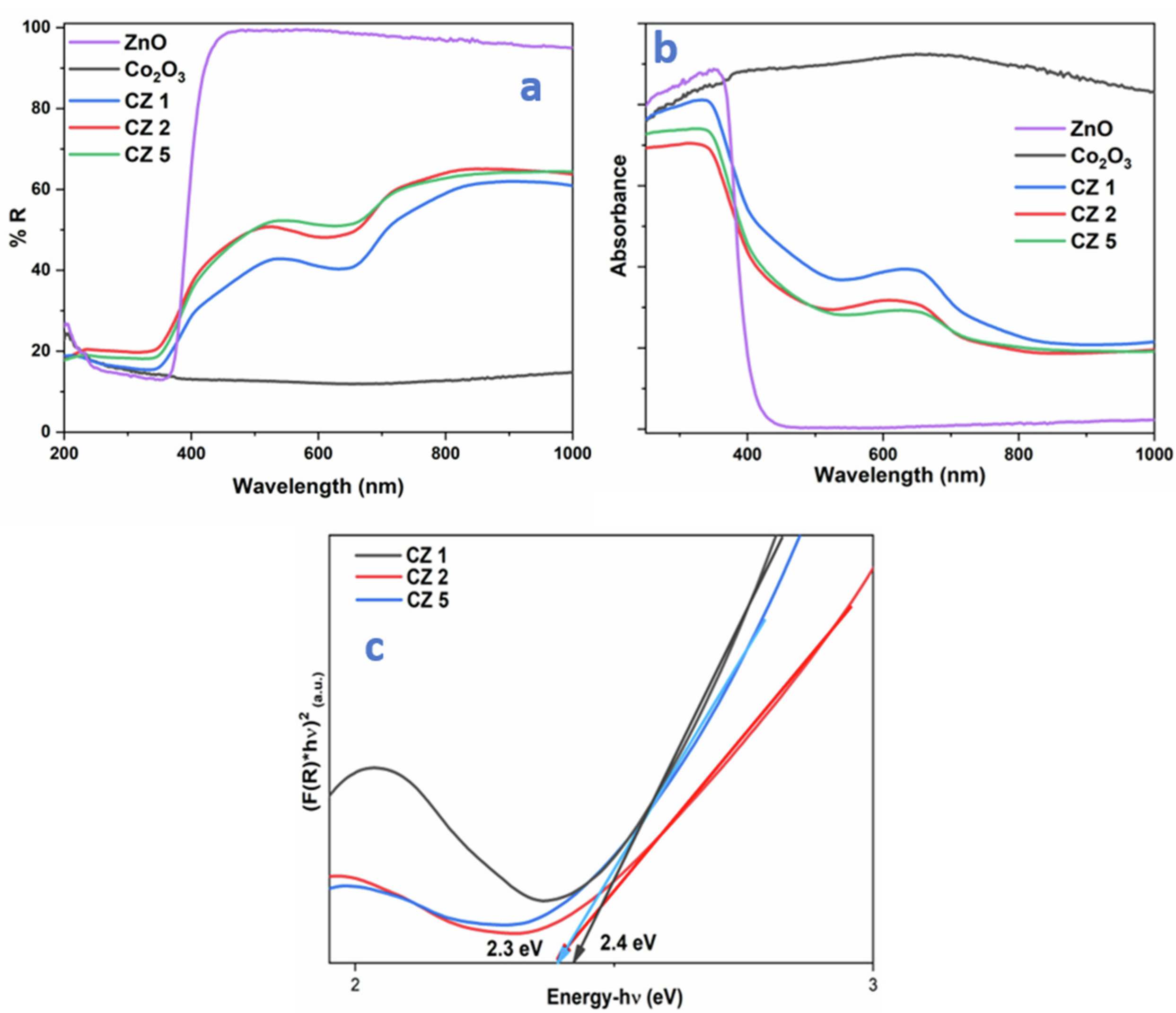

Fig. 5. Optical spectra measurements of CZ samples (a) reflectance spectra (b) absorption spectra and (c) evaluation of bandgaps.

Using this equation (2), we plotted the energy (hν) vs F(R), the Kubelka-Munk Factor. The band gap evaluation of the nanocomposites is shown in Fig. 5(c). According to this, the band gaps were 2.4 eV for CZ1 and 2.3 eV for both CZ2 and CZ5, which are very close. From the literature studies, and from our previous results, the band gap of zinc oxide and cobalt oxide were at 3.2 and 1.5 eV, respectively[32,33]. A band gap value of 3.2 eV lies in the UV region of the electromagnetic spectrum. So, the synthesized nanocomposites decreased the band gap of the main material, zinc oxide by the addition of cobalt oxide nanoparticles through the formation of nanocomposites. This caused an extended absorption edge of the nanocomposites into visible region as we can see in the absorption spectra (Fig. 5(b)).

To identify the decay rate of the organic dye, we measured the absorbance of each sample. This method is used by following Beer-Lambert's law[34]. This law relates the absorbance with the concentration of a solution. The detailed explanation of dye decay analysis with absorbance spectra is given in the following section.

3.5. Photocatalysis

We carried out a basic dye decay during light irradiation study to check the photocatalytic effects of the nanocomposites. The problems normally occur due to the scattering of powder samples during photocatalysis was the motivation for the fabrication of thin films in this work. The results of photocatalytic studies are shown in Fig. 6. The decrease in absorbance of the best sample (CZ5) was shown in Fig. 6(a). In Fig. 6 (b), the dye decay vs time plot was given for the three samples. The photocatalytic process was analyzed for one cycle for all the samples. The graphs show that all the nanocomposite thin films performed dye decay very well and the samples CZ2 and CZ5 performed better. In the plot of decay vs time, sample CZ1 shows an abnormality because some particles or the film got into the dye solution and the nanoparticles caused the scattering of light during the absorbance measurement. The sample CZ5 showed a decay of 80%, CZ2 showed 75% and the sample CZ 1 showed 72% of dye decay in 90 min of visible light irradiation. For all the photocatalytic studies the same setup was used. The power of the solar simulator was 200 W and observed not much temperature raise during the analysis.

In our photocatalytic studies, we used an organic dye, methylene blue. It has a blue color, and it is a well-known textile dye. The textile industries exhausting the waste materials to nearby waterbodies. This will contaminate the nature[35]. The removal of textile dye from water with photocatalysts will help nature for its sustainability. For analyzing the photocatalytic dye decay, we are using the absorbance spectra of the dye-water mixture after every 15 min of solar simulator light irradiation. Initially, the solution was with blue color and as time passes the solution paled the color and the water will be purified. From the absorption measurement, we can find out the highest peak of the dye. In the case of methylene blue, it is around, 664 nm. As the photocatalytic process proceeds, the intensity of peak at 664 nm will decrease. This is represented in Fig. 6(a). Earlier we mentioned that the absorbance can be used for concentration studies with the help of Beer-Lambert's law. The law is given below[36].

$$Decay\ percentage = \frac{C_0 - C_t}{C_0} \times 100 \tag{3}$$

In the above equation, C_0 represents the initial concentration (in terms of intensity values/ y-axis value corresponds to 664 nm), C_t represents the concentration at a specific time, t. Using this equation, the plot in Fig. 6(b) is given.

In the case of CZ1, the morphology appeared like agglomerated one, this could reduce the surface area of the material, so resulting in lesser active sites for photocatalysis. In CZ2 the morphology appeared petals like structure, also appeared with some independent particles on the surface. This can act better than CZ1 due to the higher surface area than CZ1. In the case of CZ5, the morphology looks like a combination of spherical and needle forms of particles. This surface morphology could provide a more active surface area than that of CZ1 and CZ2. From the XPS results, more oxygen contribution was also observed for the sample CZ5 which could provide more active oxygen radicals for dye degradation. It was observed that the CZ5 sample surface has oxygen contribution from both the metallic oxides.

This work shows the modified morphology and optical properties of $ZnO:Co_2O_3$ nanocomposites by pulsed laser irradiation in liquid, which will be helpful for the tuning of oxide nanomaterials morphologies and optoelectronic properties. In SEM images the morphology observed a gradual alteration towards spherical structures. In optical studies, the band gap observed value of 2.4 eV which can absorb more visible radiation from the solar spectrum. The XPS analysis also showed a gradual enhancement in cobalt

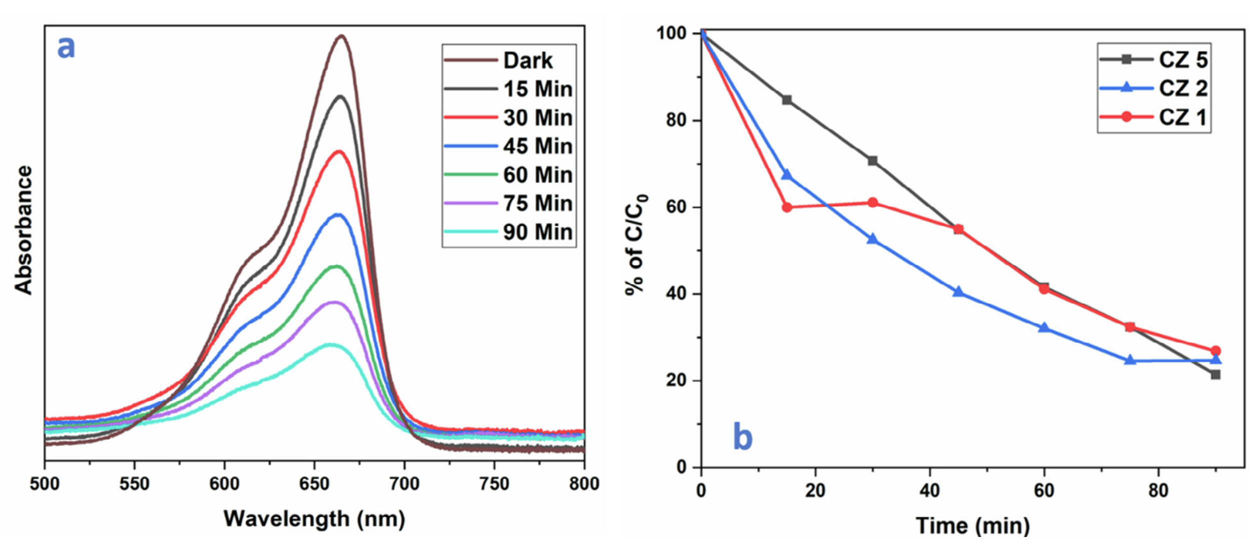

Fig. 6. (a) Dye decay absorption measurement for sample CZ5. (b) percentage of methylene blue dye decay with respect to different time intervals. (For interpretation of the references to color in this figure legend, the reader is referred to the web version of this article.)

content and a difference in oxygen high resolution spectra in accordance with the percentage change of cobalt oxide. As future work, to improve the photocatalytic performance, the synthesis part can be easily modified to obtain other nanocomposites with enhanced visible light absorption, lower band gaps, or their hybrids with metal nanoparticles by this technique.

4. Conclusions

In this work, we synthesized zinc oxide-cobalt oxide nanocomposites with pulsed laser irradiation in liquid technique. The total time for the synthesis of these nanocomposites was below 1 h. The final product quantity was also very high, a minimum of 30 mg. According to the varying concentration of cobalt oxide in the nanocomposites, we observed changes in the morphology, optical, and photocatalytic properties. From the morphological analysis, we observed the morphology tends to spherical in shape for higher cobalt oxide concentration. Optical bandgap was in the visible range that helped for visible light photocatalytic activity. So, for optimum concentration of the composite with appropriate irradiation time has a chance to give perfect spherical structures, which favors high photocatalytic activity by providing more surface area, so that more contribution to active sites for photocatalysis. Another important finding is the preparation of uniform thin films from the nanocolloid and their use as photocatalysts.

Declaration of Competing Interest

The authors declare that they have no known competing financial interests or personal relationships that could have appeared to influence the work reported in this paper.

Acknowledgments

Sreed Sharma Kanakkillam is thankful to CONACYT, Mexico, for providing financial support for doctoral studies. Expressing gratitude towards graduate student Andrea Oliva, for her aids during the experimental works as a social service student from Facultad de Ciencias Biológicas, Universidad Autonoma de Nuevo Leon (UANL). Mexico.

References

[1] M.F.-G. José A. Rodríguez, SYNTHESIS, PROPERTIES, AND APPLICATIONS OF OXIDE NANOMATERIALS, 2007. https://doi.org/10.1002/0470108975.
[2] N. El-Atab, N. Qaiser, H. Badghaish, S.F. Shaikh, M.M. Hussain, Flexible Nanoporous Template for the Design and Development of Reusable Anti-COVID-19 Hydrophobic Face Masks, ACS Nano 14 (6) (2020) 7659–7665.
[3] J. PORTIER, H. HILAL, I. SAADEDDIN, S. HWANG, M. SUBRAMANIAN, G. CAMPET, Thermodynamic correlations and band gap calculations in metal oxides, Prog. Solid State Chem. 32 (3-4) (2004) 207–217.
[4] G.G. Guillén, M.I.M. Palma, B. Krishnan, D. Avellaneda, G.A. Castillo, T.K.D. Roy, S. Shaji, Structure and morphologies of ZnO nanoparticles synthesized by pulsed laser ablation in liquid: Effects of temperature and energy fluence, Mater. Chem. Phys. 162 (2015) 561–570.
[5] G.G. Guillén, S. Shaji, M.I.M. Palma, D. Avellaneda, G.A. Castillo, T.K.D. Roy, D.I. G. Gutiérrez, B. Krishnan, Effects of ablation energy and post-irradiation on the structure and properties of titanium dioxide nanomaterials, Appl. Surf. Sci. 405 (2017) 183–194.
[6] A. Šutka, T. Käämbre, R. Pärna, I. Juhnevica, M. Maiorov, U. Joost, V. Kisand, Co doped ZnO nanowires as visible light photocatalysts, Solid State Sci. 56 (2016) 54–62.
[7] M.K. Lima, D.M. Fernandes, M.F. Silva, M.L. Baesso, A.M. Neto, G.R. de Morais, C. V. Nakamura, A. de Oliveira Caleare, A.A.W. Hechenleitner, E.A.G. Pineda, Co-doped ZnO nanoparticles synthesized by an adapted sol–gel method: effects on the structural, optical, photocatalytic and antibacterial properties, J Sol-Gel Sci Technol 72 (2) (2014) 301–309.
[8] R. Saravanan, S. Karthikeyan, V.K. Gupta, G. Sekaran, V. Narayanan, A. Stephen, Enhanced photocatalytic activity of ZnO/CuO nanocomposite for the degradation of textile dye on visible light illumination, Mater. Sci. Eng., C 33 (1) (2013) 91–98.
[9] C.V. Niveditha, M.J. Jabeen Fatima, R. Ramanarayanan, S. Swaminathan, Size Control through Scan Rate Modulation: Mapping Water Splitting Efficiency of Micro to Nano Size Cuboidal Copper Oxide Particles, J. Electrochem. Soc. 165 (14) (2018) H908–H915.
[10] S.S. Kanakkillam, S. Shaji, B. Krishnan, S. Vazquez-Rodriguez, J.A.A. Martinez, M.I.M. Palma, D.A. Avellaneda, Nanoflakes of zinc oxide:cobalt oxide composites by pulsed laser fragmentation for visible light photocatalysis, Appl. Surf. Sci. 501 (2020) 144223, https://doi.org/10.1016/j.apsusc.2019.144223.
[11] J. Johny, S. Sepulveda-Guzman, B. Krishnan, D.A. Avellaneda, J.A. Aguilar Martinez, S. Shaji, Synthesis and Properties of Tin Sulfide Thin Films from Nanocolloids Prepared by Pulsed Laser Ablation in Liquid, ChemPhysChem 18 (9) (2017) 1061–1068.
[12] J. Taha-Tijerina, S. Shaji, S.S. Kanakkillam, M.I.M. Palma, K. Aviña, Tribological and thermal transport of Ag-vegetable nanofluids prepared by laser ablation, Appl. Sci. 10 (2020) 1–12, https://doi.org/10.3390/app10051779.
[13] M.I. Mendivil, B. Krishnan, F.A. Sanchez, S. Martinez, J.A. Aguilar-Martinez, G.A. Castillo, D.I. Garcia-Gutierrez, S. Shaji, Synthesis of silver nanoparticles and antimony oxide nanocrystals by pulsed laser ablation in liquid media, Appl. Phys. A 110 (4) (2013) 809–816.
[14] V.A. Zuñiga-Ibarra, S. Shaji, B. Krishnan, J. Johny, S. Sharma Kanakkillam, D.A. Avellaneda, J.A.A. Martinez, T.K.D. Roy, N.A. Ramos-Delgado, Synthesis and characterization of black TiO2 nanoparticles by pulsed laser irradiation in liquid, Appl. Surf. Sci. 483 (2019) 156–164.
[15] S.S. Kanakkillam, B. Krishnan, D.A. Avellaneda, S. Shaji, Surfactant free stable cobalt oxide nanocolloid in water by pulsed laser fragmentation and its thin films for visible light photocatalysis, Colloids Surf., A 594 (2020) 124657, https://doi.org/10.1016/j.colsurfa.2020.124657.
[16] N.M. Bedford, A.J. Steckl, Photocatalytic Self Cleaning Textile Fibers by Coaxial Electrospinning, ACS Appl. Mater. Interfaces 2 (8) (2010) 2448–2455.
[17] S.A. Asif, S. Khan, A.M. Asiri, Efficient solar photocatalyst based on cobalt oxide/iron oxide composite nanofibers for the detoxification of organic pollutants, Nanoscale Res Lett 9 (1) (2014) 510, https://doi.org/10.1186/1556-276X-9-510.
[18] B.N. Meethal, N. Pullanjiyot, S. Swaminathan, Anchoring of polymeric precursor on oxygen deficient ZnO nanotubes: A chelation assisted combined nucleation-growth-dissolution synthesis strategy, Mater. Des. 130 (2017) 426–432.
[19] S. Filice, G. Compagnini, R. Fiorenza, S. Scirè, L. D'Urso, M.E. Fragalà, P. Russo, E. Fazio, S. Scalese, Laser processing of TiO2 colloids for an enhanced photocatalytic water splitting activity, J. Colloid Interface Sci. 489 (2017) 131–137.
[20] H. Yuan, S.A.A.A. Aljneibi, J. Yuan, Y. Wang, H. Liu, J. Fang, C. Tang, X. Yan, H. Cai, Y. Gu, S.J. Pennycook, J. Tao, D. Zhao, ZnO Nanosheets Abundant in Oxygen Vacancies Derived from Metal-Organic Frameworks for ppb-Level Gas Sensing, Adv. Mater. 31 (11) (2019) 1807161, https://doi.org/10.1002/adma.v31.1110.1002/adma.201807161.
[21] P.V. Laxma Reddy, B. Kavitha, P.A. Kumar Reddy, K.-H. Kim, TiO 2 -based photocatalytic disinfection of microbes in aqueous media: A review, Environ. Res. 154 (2017) 296–303.
[22] N. Negishi, C. Chawengkijwanich, N. Pimpha, S. Larpkiattaworn, T. Charinpanitkul, Performance verification of the photocatalytic solar water purification system for sterilization using actual drinking water in Thailand, J. Water Process Eng. 31 (2019) 100835, https://doi.org/10.1016/j.jwpe.2019.100835.
[23] M. Pelaez, N.T. Nolan, S.C. Pillai, M.K. Seery, P. Falaras, A.G. Kontos, P.S.M. Dunlop, J.W.J. Hamilton, J.A. Byrne, K. O'Shea, M.H. Entezari, D.D. Dionysiou, A review on the visible light active titanium dioxide photocatalysts for environmental applications, Appl. Catal. B 125 (2012) 331–349.
[24] P. Ganguly, M. Harb, Z. Cao, L. Cavallo, A. Breen, S. Dervin, D.D. Dionysiou, S.C. Pillai, 2D Nanomaterials for Photocatalytic Hydrogen Production, ACS Energy Lett. 4 (7) (2019) 1687–1709.
[25] J. Podporska-Carroll, A. Myles, B. Quilty, D.E. McCormack, R. Fagan, S.J. Hinder, D.D. Dionysiou, S.C. Pillai, Antibacterial properties of F-doped ZnO visible light photocatalyst, J. Hazard. Mater. 324 (2017) 39–47.
[26] D. Zhang, Z. Yang, Z. Wu, G. Dong, Metal-organic frameworks-derived hollow zinc oxide/cobalt oxide nanoheterostructure for highly sensitive acetone sensing, Sens. Actuators, B 283 (2019) 42–51.
[27] R.M. Mohamed, D. McKinney, M.W. Kadi, I.A. Mkhalid, W. Sigmund, Cobalt/zinc oxide hollow spheres: Visible light nanophotocatalysts, Ceram. Int. 42 (2) (2016) 2299–2305.
[28] E.H.H. Hasabeldaim, O.M. Ntwaeaborwa, R.E. Kroon, E. Coetsee-Hugo, H.C. Swart, Pulsed laser deposition of a ZnO:Eu3+ thin film: Study of the luminescence and surface state under electron beam irradiation, Appl. Surf. Sci. 502 (2020) 144281, https://doi.org/10.1016/j.apsusc.2019.144281.
[29] J.Y. Choi, C.K. Lim, B. Park, M. Kim, A. Jamal, H. Song, Surface activation of cobalt oxide nanoparticles for photocatalytic carbon dioxide reduction to methane, J. Mater. Chem. A 7 (25) (2019) 15068–15072.

[30] K.R. Nandanapalli, D. Mudusu, J.-S. Yu, S. Lee, Stable and sustainable photoanodes using zinc oxide and cobalt oxide chemically gradient nanostructures for water-splitting applications, J. Colloid Interface Sci. 558 (2020) 9–20.
[31] A. Sahai, Y. Kumar, V. Agarwal, S.F. Olive-Méndez, N. Goswami, Doping concentration driven morphological evolution of Fe doped ZnO nanostructures, J. Appl. Phys. 116 (16) (2014) 164315, https://doi.org/10.1063/1.4900721.
[32] J. Wang, R. Chen, L. Xiang, S. Komarneni, Synthesis, properties and applications of ZnO nanomaterials with oxygen vacancies: A review, Ceram. Int. 44 (7) (2018) 7357–7377.
[33] T. Warang, N. Patel, R. Fernandes, N. Bazzanella, A. Miotello, Co3O4 nanoparticles assembled coatings synthesized by different techniques for photo-degradation of methylene blue dye, Appl. Catal. B 132-133 (2013) 204–211.
[34] L. Buzzetti, G.E.M. Crisenza, P. Melchiorre, Mechanistic Studies in Photocatalysis, Angew. Chem. Int. Ed. 58 (12) (2019) 3730–3747.
[35] K. Jalali, E. Pajootan, H. Bahrami, Elimination of hazardous methylene blue from contaminated solutions by electrochemically magnetized graphene oxide as a recyclable adsorbent, Adv. Powder Technol. 30 (10) (2019) 2352–2362.
[36] F. Shen, W. Que, Y. He, Y. Yuan, X. Yin, G. Wang, Enhanced Photocatalytic Activity of ZnO Microspheres via Hybridization with CuInSe 2 and CuInS 2 Nanocrystals, ACS Appl. Mater. Interfaces 4 (8) (2012) 4087–4092.